Double acting composite tube cylinder for fluid power applications: a design procedure

S. Mantovani & D. Costi
MilleChili Lab
Università degli Studi di Modena e Reggio Emilia
Modena, Italy
sara.mantovani@unimore.it

A. Strozzi & E. Bertocchi
Facoltà Ingegneria
Università degli Studi di Modena e Reggio Emilia
Modena, Italy

E. Dolcini
Research & Development
RI-BA Composites Srl
Faenza, Italy
edolcini@ribacomposites.it

Abstract — **A preliminary study on a double acting hydraulic cylinder is described. This research explores the design method to replace the steel cylinder tube with carbon composite materials. The composite cylinder must satisfy the same steel cylinder performance like maximum operating pressure, buckling load, modal behaviour and seals' deformation. MilleChili Lab and RI-BA Composites Srl are exploring lightweight options to steel. Composite materials are an alternative for structural applications in terms of saving weight policy. Composite lay-up design and product geometry take account of composite manufacturing process for a relatively high volume production. The present paper describes the guidelines for designing non conventional hydraulic cylinder using finite element method, Lamè solution and composite theory.**

Keywords-hydraulic cylinder double acting; carbon composite material; buckling load; modal analysis; finite element method

I. Introduction

Hydraulic cylinders used in the mechanical and civil engineering fields are usually made of traditional metals. High Strength Steel (HSS) is normally used for the rod and the cylinder tube whereas the pistons are normally made of aluminum. In mobile application such as naval, railway and aerospace, weight is crucial and it is therefore a major design criteria. The use of novel composite materials therefore offers a valuable alternative. The main aspects of the hydraulic cylinder design are described in several manuals and books, i.e. Hunt *et al.* [1] and Speich *et al.* [2], which provide guidelines for successful design of such components. These manuals provide a comprehensive scenario of problems and targets that must be considered during the design. In the last few years, buckling analysis and tribology problems between ring seal piston and cylinder were investigated extensively. Baragetti *et al.* [3] presented numerical models to analyse the buckling behaviour of a double acting cylinder. His analytical and experimental model studied friction and imperfections between piston and rod-cylinder connections. In a subsequent work, Gamez-Montero *et al.* [4] evaluated the buckling instability considering initial misalignment as an imperfection in the rod-cylinder tube intersection. Their research defined the influence of the misalignment angle on buckling load by both numerical and experimental approaches. Several other works [5–6] consider stroke and cushioning devices to reduce the piston-rod kinetic energy during motion. They also formed a mathematical model of hydraulic circuits to study the supply pressure influence, and they evaluated alternative solutions. Thin-walled composite cylinders are studied for mechanical applications such as pressure vessels [7–10] and car crash energy absorbers [11]. In the last years, composite materials have been applied in pressure vessels applications as chemicals storage [8–9]. The coupling of an inner liner with composite laminates is designed to contain gas under high pressure, to avoid the composite material corrosion and occasionally, to carry part of the load. In [11], buckling behaviour of cylinder composite material was developed by numerical and experimental correlation using Finite Element Method (FEM). Optimization techniques have been applied to cylinder composite stacking sequence and shape in order to increase the critical buckling load and to dissipate the major amount of energy due to dynamic stresses. Unfortunately, the possibility of using composite materials has not been studied for applications in hydraulic cylinders as many authors did not take into consideration their advantages. The aim of this work is to evaluate a weight efficient alternative design of an hydraulic tube cylinder in a double acting actuator using carbon composites. This work is comprised of five steps. In the first step, the reference steel actuator is analysed. In the second step, the a Lamé solution [12] has been obtained for orthotropic materials, and formulas developed for composite thick-walled cylinder stresses and strains. In the third and forth step, the thickness of composite cylinder tube is calculated by evaluating the required circumferential and axial load bearing requirements. In the last step advanced topics like buckling and

TABLE I. WEIGHT OF THE REFERENCE HYDRAULIC CYLINDER PARTS

Component	Material	Weight [kg]	% Weight
Piston	Aluminum	24	3%
Rod	Steel	320	40%
Joint	Aluminum	55	7%
Cylinder Tube	Steel	410	51%
Total Weight		809 kg	

TABLE II. REFERENCE CYLINDER TUBE STRESS AT FIRST-YIELD

Reference cylinder tube	
p_i	67 MPa
$\sigma_\theta\|_{r=ri}$	483 MPa
$u\|_{r=ri}$	0,359 mm

dynamic behaviour are discussed comparing the original solution and the composite replacement.

II. METHOD

A. Step 1: reference case analysis

The reference hydraulic cylinder tube was 300 mm in bore diameter, 23 mm in thickness and 2250 mm in length. The nominal operating pressure was 35 MPa. As in Table I, the cylinder tube represents the 51% of the overall hydraulic actuator weight in the reference configuration. The internal yield pressure (p_i) of the steel cylinder tube has been calculated using the Lamé solution for thick-walled vessels; the circumferential stress ($\sigma_\theta|_{r=ri}$) and the radial displacement ($u|_{r=ri}$) at the inner cylinder radius were accordingly evaluated. Results are shown in Table II.

The first-yield condition represents a soft failure mode that precedes the catastrophic failure of the component, which is associated to the full-yielded state at burst pressure. The former limit state rather than the latter has been chosen for the following comparative safety analyses since the structural steel yielding phase has only a weak counterpart in FRP materials. Besides that, limiting the analyses below the first-yield threshold allows considerations based on linearity.

B. Step 2: Lamé solution for orthotropic materials

Material composite stiffness properties depends on the reinforcement orientation and on reinforcement volume fraction. For a unidirectional composite ply, a scale factor λ between the Young's modulus in the principal reinforcement direction E_1 and the transversal one E_2 can be defined as

$$\lambda^2 = \frac{E_1}{E_2} \tag{1}$$

Solving equilibrium and compliance equations under the plane stress hypothesis, the radial displacement u(r) of thick-walled composite vessel as a function of radial position r:

$$u(r) = C_1 r^{-\frac{1}{\lambda}} + C_2 r^{\frac{1}{\lambda}} \tag{2}$$

The constants C_1 and C_2 can be calculated by considering the cylinder radial stress (σ_r) respectively at the inner cylinder radius (r_i) and at the outer radius (r_e).

$$\begin{aligned} \sigma_r \,|_{r=r_i} &= -p_i \\ \sigma_r \,|_{r=r_e} &= 0 \end{aligned} \tag{3}$$

$$\begin{aligned} C_1 &= -\frac{r_i \cdot p_i \cdot r_e^{\frac{1}{\lambda}} \cdot (\upsilon_{12} \cdot \lambda + 1)}{\lambda \cdot E_1 \cdot \left(r_e^{-\frac{1}{\lambda}} \cdot r_i^{\frac{1}{\lambda}} - r_i^{-\frac{1}{\lambda}} \cdot r_e^{\frac{1}{\lambda}} \right)} \\ C_2 &= \frac{r_i \cdot p_i \cdot r_e^{-\frac{1}{\lambda}} \cdot (\upsilon_{12} \cdot \lambda - 1)}{\lambda \cdot E_1 \cdot \left(r_e^{-\frac{1}{\lambda}} \cdot r_i^{\frac{1}{\lambda}} - r_i^{-\frac{1}{\lambda}} \cdot r_e^{\frac{1}{\lambda}} \right)} \end{aligned} \tag{4}$$

where the ν_{12} is the Poisson's ratio of the composite ply. The circumferential stress (5) and the radial displacement at the inner cylinder diameter (6) can be expressed as:

$$\sigma_\theta \,|_{r=r_i} = \frac{\left(r_e^{\frac{2}{\lambda}} \cdot r_i^{-\frac{1}{\lambda}} + r_i^{\frac{1}{\lambda}} \right) \cdot r_i^{\frac{1}{\lambda}} \cdot p_i}{\lambda \cdot \left(-r_i^{\frac{2}{\lambda}} + r_e^{\frac{2}{\lambda}} \right)} \tag{5}$$

$$u_r \,|_{r=r_i} = \frac{p_i \cdot r_i \cdot \left(r_e^{\frac{2}{\lambda}} \cdot \nu_{12} \cdot \lambda + r_e^{\frac{2}{\lambda}} - r_i^{\frac{2}{\lambda}} \cdot \nu_{12} \cdot \lambda + r_i^{\frac{2}{\lambda}} \right)}{\lambda \cdot E_1 \cdot \left(-r_i^{\frac{2}{\lambda}} + r_e^{\frac{2}{\lambda}} \right)} \tag{6}$$

Finally, the outer radius can be calculated as a function of the radial displacement at inner radius and of the inner radius itself as follows:

$$r_e = \left(\frac{\frac{u_r \,|_{r=r_i}}{r_i} \cdot \lambda \cdot E_1 + p_i \cdot (1 - \nu_{12} \cdot \lambda)}{\frac{u_r \,|_{r=r_i}}{r_i} \cdot \lambda \cdot E_1 + p_i \cdot (-1 - \nu_{12} \cdot \lambda)} \right)^{\frac{\lambda}{2}} \cdot r_i \tag{7}$$

TABLE III. REINFORCEMENT PROPERTIES

Carbon fiber type	Tensile Modulus	Tensile strenght	Density
	[MPa]	*[MPa]*	*[g/cm3]*
Intermediate Modulus (IM)	300000	5500	1.80
High Modulus (HM)	440000	4200	1.85
Ultra High Modulus (UHM)	620000	3500	2.10

TABLE IV. MATRIX PROPERTIES

Matrix	Tensile Modulus	Tensile strenght	Density
	[MPa]	*[MPa]*	*[g/cm3]*
Epoxy Matrix (EM)	3800	/	1.22

C. Step 3: Design for pressurized fluid radial retention

Both the circumferential and the axial stresses on cylinder tube must taken into consideration while defining composite materials stacking sequence. In the present work, three unidirectional continuous reinforcements and an epoxy matrix have been considered; elastic and strength properties for selected materials are shown in Table III and IV.

The cylinder composite lay-up includes both plies at 90° – normal to cylinder axis – to hold the circumferential stresses, and 0° plies to bear the axial stress. In the current paragraph the circumferentially oriented portion of the laminate stack are considered, whereas the axially oriented portion is covered in the following one. The main design constraint for 90° plies total thickness is the circumferential stress value at inner tube radius. Since the tensile allowed stress to stiffness ratio is higher in CFRP than in construction steels, designing the cylinder tube on the limit of its mechanical resistance leads to substantially higher radial deformation under load. Unlike in similar applications like pressure vessels and gas bottles, an increased radial expansion in hydraulic cylinders can cause both seal leakage and piston misalignment due to gap at bearing bands. Limiting the radial displacement at the tube inner radius to an admissible value becomes a second design constraint. The inner surface of the composite tube – although laid in direct contact with the mold – is tribologically unsuitable to pair seals and bearing bands in sliding contact. The insertion of a thin steel liner was therefore considered for such purposes. Whereas neglected in calculations as a reinforcing element, the bonded liner imposes a third design constraint in terms of admissible circumferential and axial strains at the tube inner surface. Being the liner a non load-bearing element which relies on the outer composite layers for support, its yielding can be tolerated as long as strain induced fractures do not appear. Such condition evidently imposes that the equivalent strain remains below the material elongation at break, however a usually stricter constraint can be found in avoiding cyclical hysteretic plastic loops and consequent low-cycle fatigue fractures. Being the steel layer supposed infinitesimally thin, it inherits its circumferential and axial strain values from the composite layer it is bound to. As pointed out in the elastic-perfectly plastic stress strain curve in Fig. 1, a limit peak strain value (ε_{lim}) exists such that, besides a

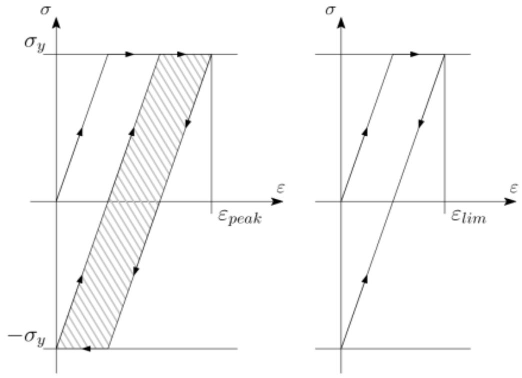

Figure 1. Deformation cycle for liner – composite assembly.

first-cycle yielding, following loading and unloading cycles do not cause further plastic deformations. Such strain value is associated to the limit condition of a null-area hysteretic loop, and can be evaluated as

$$\varepsilon_{lim} = 2 \cdot \frac{\sigma_y}{E} \tag{8}$$

A comparison between the different composite materials for the radial displacement at the inner cylinder tube is presented in Fig. 2. Only the UHM fiber reach the radial stiffness of the reference steel cylinder tube, with the feasible wall thicknesses of 13 mm. The condition which bounds the minimal thickness of the composite tube (at the point marked with a 45° cross) is the allowed liner circumferential strain, whereas the thickness of the steel tube is limited by its yielding (σ_y). Considering the actual example, in the case of UHM fiber the minimum 90° plies thickness required for bearing the inner pressure is 5.3 mm, whereas the original steel wall thickness was 23 mm. The steel manufacturing process we considered allows the production of steel liner of 2 mm as minimum thickness. This becomes the forth design constraint of composite cylinder design, which impacts directly on its weight.

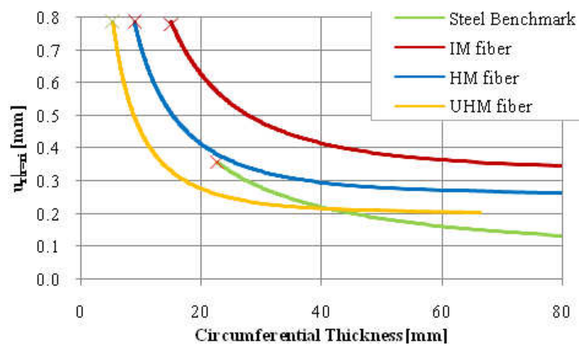

Figure 2. Radial displacement at inner radius vs. wall thickness at first-yield pressure.

D. Step 4: design for axial load retention

In the considered assembly, axial load (P_a) is due to pressure acting on the head while pulling, or on the pushing piston when retained at full stroke in absence of position limiting valves. Such loads can be respectively evaluated as

$$P_a = p_i \cdot \left(r_i^2 - r_r^2\right) \cdot \pi \tag{9}$$

or as

$$P_a = p_i \cdot r_i^2 \cdot \pi \tag{10}$$

where r_r is the rod radius. The 0° axially oriented plies amount is defined by the minimum cross section area $A_{0°}$ needed to not exceed material longitudinal tensile strength (σ_1). Unlike the circumferential case, the steel liner could be isolated from the composite tube axial deformation through an anti-friction coating; such solution is however impractical, and composite cylinder tube axial strain has to be limited as well in order to preserve the inner bonded steel liner. Hence the required amount of axially oriented UD plies can be calculated as follows:

$$A_{0^0} = \max\left(\frac{P_a}{\sigma_1}; \frac{P_a}{\varepsilon_{lim} \cdot E_1}\right) \tag{11}$$

Since circumferential retaining plies become less effective if stacked upon a growing thickness of material, it appears advisable to add the axial plies on outer layers. Unfortunately, due to manufacturing and technological constraints, circumferential and axial UD plies has to be alternated, or an unbalanced fabric has to be used. The required axial ply thickness was evaluated in 2 mm using the UHM fiber. The composite cylinder tube is therefore composed of 2 mm of steel liner and 7.3 mm UHM UD plies in lieu of 23 mm of steel shell as in the reference assembly.

E. Step 5: advanced considerations, buckling and dynamic modal targets

As discussed above, the composite cylinder tube allows a greater radial expansion than its steel counterpart, especially when wall thickness is kept minimal and UHM fiber is not used; such compliance reduces the effectiveness of the piston bearing bands and sealing. However, the pressure asymmetry has to be taken into account since only one chamber a time is pressurized. Such condition was analyzed with simplified Finite Element analyses which shown an S-shaped wall deformation centred at the sealing point, with small overshoots due to the plate bending stiffness. As in Fig. 3, in which the pressurize chamber appears on the right, radial deformation decreases asymptotically up to zero moving within the unloaded portion, and increases up to the value returned by the Lamé solution moving within the loaded portion. It clearly appears that the sealing acts on a cylinder section at which radial deformation is half the asymptotic value. Moreover,

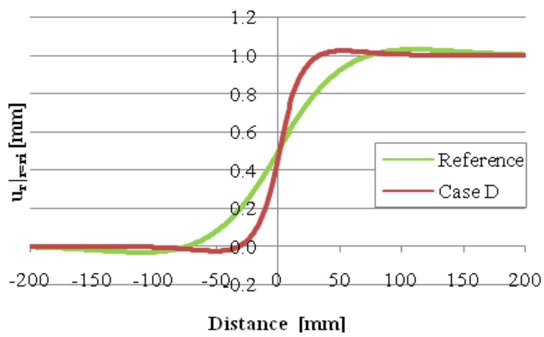

Figure 3. Relative radial deformation versus distance from the sealing point

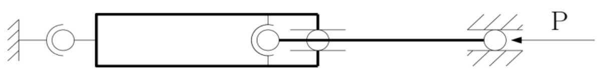

Figure 4. Buckling FE model.

TABLE V. TEST CASES STUDIED FOR COMPOSITE CYLINDER TUBE

	Amount of plies of a given kind introduced in the stacking sequence [mm]			
Case	***0°***	***90°***	***45°/-45°***	***steel liner***
A	2	5.3	/	/
B	2	5.3	/	2
C	2	5.3	2	2
D	2	5.3	4	2

radial inflation decreases more rapidly in the composite test case; the piston bearing band on the unloaded side pairs an almost undeformed cylinder section. Axially oriented UD plies also contribute in defining the buckling response of the actuator. Historically, analytical and experimental investigations were developed to study the critical buckling load of hydraulic cylinders. In the present paper, the hydraulic cylinder was modelled in analogy with the approach proposed in ISO Standards [14] and based on Hoblit's method [13]. However, a Finite Element analysis was used in place of the analytical formula in order to take into account the virtually relevant shear deflection of the composite tube. Moreover, the norm assumes that the axial load is transmitted through the tube during the pushing action, whilst in normal operation such load is supported by the constrained fluid, and the composite barrel is relieved from compressive load, retarding buckling incipience. Comparative analyses were however conducted following the norm approach, which can be pragmatically described as a seized piston condition. The mounting case method was pin-mounted hydraulic cylinder, and the relative boundary conditions are schematized in Fig. 4. It worth to be noted that the actuator rod is laterally supported by the cylinder in correspondence of the head cap bearing and at piston midpoint; axial load is transmitted from the rod end to the cylinder end. The cylinder tube was modelled by bilinear, four-node shell elements whilst beam elements were used for the piston rod. Both shell and beam elements formulation included

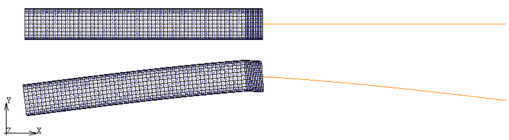

Figure 5. FE model for buckling critical load, case A.

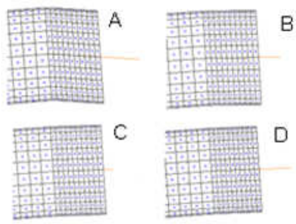

Figure 6. Local buckling deformation of the composite cylinder tube for the different test cases.

TABLE VI. BUCKLING LOAD RESULTS

	Thickness	Weight	Critical Pressure
Case	***[mm]***	***[kg]***	***[MPa]***
A	7.3	30	18.4
B	9.3	64	43.8
C	11.3	77	48.9
D	13.3	81	51.1
Reference	23.0	410	60.3

transverse shear effects. Stacking sequence has been defined by homogeneously spreading along the thickness the calculated ply amount for each fiber orientation as in Table V. The steel layer is inserted at inner radius, and was removed in test case A for comparison. It appears evident from Fig. 6 that in the case of the bare 0°/90° lamination, a local and critical shear deformation occurs between the two rod support points, significantly lowering the buckling critical load respect to the reference steel assembly.

This local deformation might has been controlled and reduced by introducing plies with ±45° orientation angle and by reinstating the steel liner as shown in Fig. 5. A local outer reinforcement can be introduced as well. Even if more 0° and ±45° plies were required in order to reach the reference cylinder performance, the threshold between the operating pressure and the buckling condition has been evaluated as satisfactory. In order to further analyze the influence of axial load in misaligned conditions, a non linear analysis was performed which simulates the actuator loaded by its own weight in a pin mounted horizontal configuration, while pushing. Fluid weight was considered as well. The bending stress (σ_{Mf}) and axial stress (σ_N) value of the rob were calculated by respectively the bending moment and the axial force on steel rod (Table VII). The assembly with the composite cylinder presents a lower bending stress value, showing that the decrease in bending stiffness – raised by the buckling analysis above – is compensated by the reduced weight. Stress increase due to misaligned axial load appear relatively small as well. Finally, a dynamic modal analysis of the hydraulic cylinder was performed to comparatively evaluate the lateral modal response of the structure. The best stacking composite sequence calculated for the buckling critical situation is evaluated for the modal analysis and it is illustrated in Table VIII.

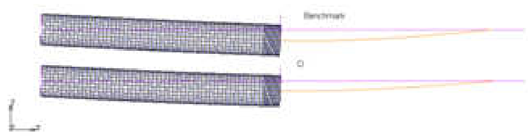

Figure 7. Deformed configuration of the cylinder tube, while pushing under it his own weight.

TABLE VII. STRESS VALUES ON THE ROD

	σ_{Mf}	σ_N
	[MPa]	***[MPa]***
Case D	±8.5	-261.3
Reference	±12.8	-261.3

TABLE VIII. MODAL ANALYSIS RESULTS

	Thickness	Weight	1st bending mode frequency
	[mm]	***[kg]***	***[Hz]***
Case D	13.3	81	18.14
Reference	23.0	410	17.28

The FE simulation shows that the composite has a higher frequency than the steel cylinder one, since the reduced inertia effect compensates the loss in stiffness.

III. Conclusions

This paper explains a method suitable for designing double-acting hydraulic cylinders with cylinder barrel made of carbon-fiber composite. This material allows significant weight saving. Weight indeed is a key feature in various structural applications. Reference properties has been calculated using the Lamé solution for thick-walled vessels. The equivalent composite cylinder tube and its optimized stacking sequence was evaluated considering separately each component of the stress tensor the cylinder is subjected to. The hoop stress depends only on the internal pressure, and so does the number and thickness of the circumferential plies. A comparison between different carbon fiber showed that the UHM fiber are the most suitable for this specific application. While resistance mainly depends on the carbon reinforcement, strain are reduce by a proper sizing of the steel liner. The smallest feasible thickness for the liner is 2 mm due to technological and manufacturing limitation. Axial stress are caused by the internal pressure and bending effects. While the total thickness depends on the total amount of axial stress, the reciprocal arrangement between the plies at 0° and 90° is due to technological constrains. With respect to the buckling behaviour, four composite stacking sequence have been compared to the reference making finite element simulations. The results of Case D, that feature also 45°/-45° plies to confine local deformation, are comparable with the reference. Finally it was assessed the equivalence of the composite cylinder with the reference for the modal analysis. The weight saving for the cylinder assembly using composite material instead of steel is above 330 kg, ensuring the same structural performances. Further improvements should deal with the piston-rod which affect about 40% of the overall weight of the cylinder assembly.

Acknowledgment

The authors are grateful to A. Bedeschi, A. Baldini, O. Masood for their technical support during the development of the present research.

References

[1] T. Hunt, and N. Vaughan, The hydraulic handbook, 9th ed., Elsevier advanced technology, 1996.

[2] H. Speich, and A. Bucciarelli, Manuale di oleodinamica. Principi, componenti, circuiti, applicazioni, Tecniche Nuove, 2002.

[3] S. Baragetti, and A. Terranova, "Bending behaviour of double-acting hydraulic actuator," Proceeding of the Institution of Mechanical Engineers, Part C: Journal of Mechanical and Engineering Sciences, vol. 215, pp. 607–619, 2001.

[4] P. J. Gamez-Montero, E. Salazar, R. Castilla, M. Khamashta, and E. Codina, "Misalignment effects on the load capacity of a hydraulic cylinder," International Journal of Mechanical Sciences, vol. 51, pp. 105–113, 2005.

[5] T. Lie, P. J. Chapple, and D. G. Tilley, "Actuator cushion performance simulation and test results," Proceedings of Workshop on Power Transmission and Motion Control, pp. 187–198, 2000.

[6] C. Schwartz, V. J. De Negri, and J. V. Climaco, "Modeling and analysis of an auto-adjustable stroke end cushioning device for hydraulic cylinders," Journal of the Brazil Society of Mechanical Science & Engineering, vol. 27, pp. 415–425, 2005.

[7] J. M. Lifshitz, and H. Dayan, "Filament-wound pressure vessel with thick metal liner," Composite Structures, vol. 32, pp. 313–323, 1995.

[8] D. Chapelle, and D. Perreux, "Optimal design of type 3 hydrogen vessel: part I - analytic modelling of the cylindrical section," International Journal of Hydrogen Energy, vol. 31, pp. 627–638, 2006.

[9] C. Comond, D. Perreux, F. Thiebaud, and M. Weber, "Methodology to improve the lifetime of type III HP tank with a steel liner," International Journal of Hydrogen Energy, vol. 34, pp. 3077–3090, 2009.

[10] C. Thesken, P. L. N. Murthy, S. L. Phoenix, N. Greene, J. L. Palko, J. Eldridge, J. Sutter, R. Saulsberry, and H. Beeson, "A theoretical investigation of composite overwrapped pressure vessel (COPV) mechanics applied to NASA full scale tests," Composite Structures, NASA/TM 215684, 2009.

[11] C. Bisagni, G. Di Pietro, L. Fraschini, and D. Terletti, "Progressive crushing of fiber-reinforced composite structural components of a Formula One racing car," Composite Structures, vol. 68, pp. 491–503, 2005.

[12] S.P. Timoshenko, and J. N. Goodiesr, Theory of Elasticity, N.Y.: McGraw-Hill, 1970.

[13] F. Hoblit, "Critical buckling load for hydraulic actuating cylinders," Product Engineering, vol. 21, pp. 108–112, 1950.

[14] ISO/TS 13725:2001, "Hydraulic fluid power-cylinders: method for determining the buckling load".